Rotating photonic crystals: A medium for compact optical gyroscopes

Ben Zion Steinberg*
School of Electrical Engineering, Tel Aviv University, Ramat-Aviv, Tel-Aviv 69978, Israel
(Received 7 December 2004; published 31 May 2005)

The effect of rotation of a photonic crystal that contains a set of microcavities is studied using the formulation of electrodynamics in rotating media. A new manifestation of the Sagnac effect is observed. It is shown that the phase shift or frequency difference between rotation-codirected and rotation-counterdirected propagations depends on a set of parameters not previously reported. The use of the new configuration for designing compact optical gyroscopes is studied and discussed.

DOI: 10.1103/PhysRevE.71.056621 PACS number(s): 41.20.−q, 42.70.Qs, 42.25.Bs

I. Introduction

The phase accumulated by a light signal that propagates along a slowly rotating circular path depends linearly on the path's angular velocity $\mathbf{\Omega}$. This phenomenon, known as the Sagnac effect, has been studied quite extensively in the literature. The interest stems not only from the theoretical viewpoint, but also from the practical one; highly sensitive rotation measurement devices can be designed using this effect [1–3].

The purpose of the present study is to explore the effect of rotation on light that propagates along a circular path within a photonic crystal (PhC). We use the coupled cavity waveguide (CCW) [4–6]—shown in Fig. 1—as the mean for providing a controlled guiding of the light signal along the circular path, as shown schematically in Fig. 2. This specific setting has several attributes that are not present in classical studies of rotating optical systems [1–3]. The first and most significant difference stems from the basic physics associated with the propagation mechanism. In classical studies, the propagation is essentially that of a plane wave, or a fiber-optical mode, within a medium that is homogeneous along its axis; the phase accumulation is essentially of the nature of a geometrical optics ray, or a local plane wave. In contrast, the CCW is a linear array of equally spaced identical local defects, situated within an otherwise perfect PhC. Examples of CCWs are shown in Fig. 1. It is well known that each of the local defects, when isolated, forms a high-Q microcavity that can trap light at frequency ω_0 within the frequency band gap of the background perfect PhC (the trapped mode). When a set of such microcavities is situated along an array (forming the CCW), signal propagation along the CCW is based on tunneling of light from one microcavity to the next. Thus, the propagation mechanism is quite different from that of a conventional fiber or laser resonator. The second important difference lies in the dispersion relation and bandwidth associated with the CCW. The classical cases of plane waves or fiber optical modes are associated with relatively weak dispersion and large bandwidth. The CCW propagation modes, constructed via a global treatment of the local tunneling effects described above [5], possess essentially a Floquet-Bloch character (after all, the CCW is a periodic structure) and are relatively narrowband.

The specific geometry under study is shown in Fig. 2 and 3. We shall call it the *ring resonator CCW* (RR-CCW). Figure 2 shows the two CCWs of Fig. 1, folded back upon themselves, in angles that preserve the *symmetry* properties along the CCW (that is, the relative orientation of each microcavity with respect to its neighbors is preserved along the path). The total number of microcavities M is finite, where in these examples we have $M=6$. The system is at rest in the inertial frame $\mathcal{I}:(x,y,z)$.

Figure 3 shows a RR-CCW, rotating in a counterclockwise direction, at an angular velocity $\mathbf{\Omega}$ around its center. This RR-CCW is at rest in the (nonmertial) rotating reference frame $\mathcal{R}:(x',y',z')$. The main purpose of this work is to derive the system response–dispersion relations and bandwidth, in the rotating frame $\mathcal{R}$. It extends the basic idea outlined by the author in a short letter [7], provides the mathematical and technical details, and discusses the applications. We expect the dispersions in $\mathcal{R}$ of clockwise and counterclockwise propagation to differ, depending on the sign and magnitude of $\mathbf{\Omega}$. Since the system is noninertial, we shall reformulate the problem within the framework of electrody-

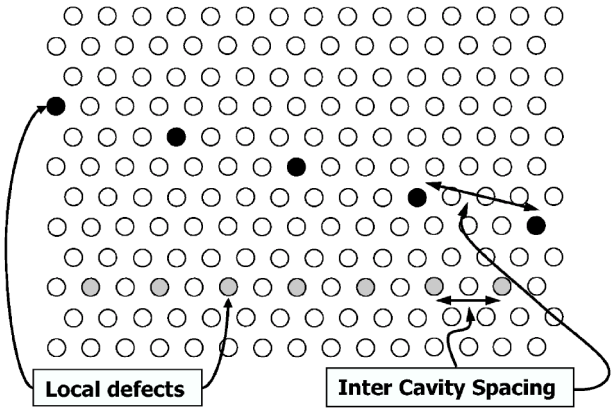

FIG. 1. Two examples of coupled cavities waveguide (CCW), in a hexagonal photonic crystal. Shaded circular domains represent local defects of a prescribed type. Filled circular domains represent yet another type of local defects. The type of local defect determines the microcavity resonant frequency ω_0, while the intercavity spacing determines the waveguide bandwidth.

*Email address: steinber@eng.tau.ac.il

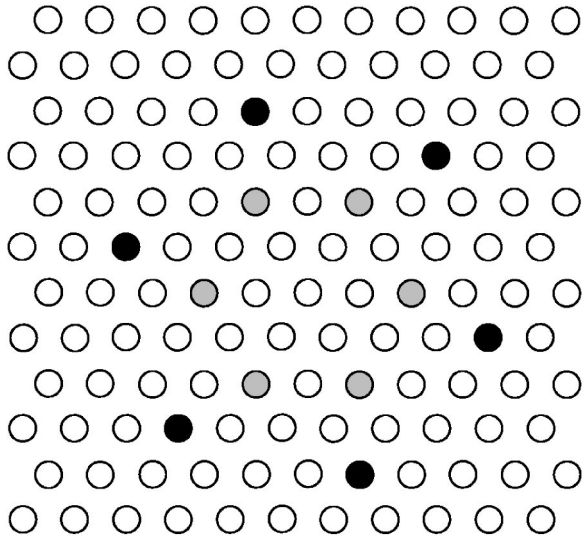

FIG. 2. Two examples of ring resonator CCWs, constructed from the linear CCWs shown in Fig. 1.

namics of accelerating or rotating systems [8,9]. This set of equations differs from the conventional set of Maxwell's equations essentially by the introduction of modified constitutive relations that depend of the angular velocity $\mathbf{\Omega}$. The resulting wave equation is no longer self-adjoint—a fact that clearly indicates, *a priori*, that clockwise and counterclockwise propagations should possess different dispersions. As we shall see, this manifestation of the Sagnac effect yields phase shifts and frequency dispersion that depend on a new set of parameters, not previously reported or studied.

Finally, we note that previous studies of accelerating or rotating photonic crystals have been reported in [10,11]. In addition, numerical studies of time-dependent PhC structures using finite difference time domain (FDTD) codes were performed, for example in [12]. In these works, interesting frequency transition effects are reported. Particularly, in [10,11] a theory is developed in which the formulation is written in the laboratory (inertial) frame of reference. However, these works do not address directly the goals articulated above. The author of the present paper believes that a formulation

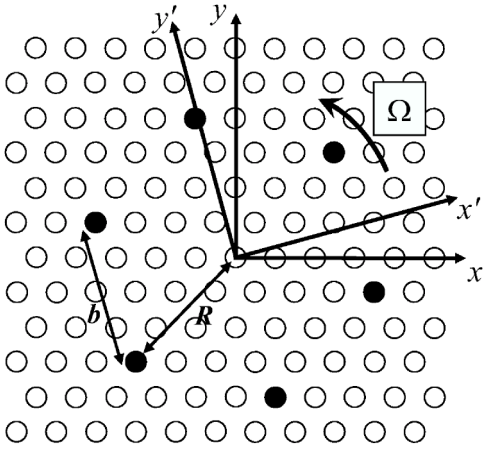

FIG. 3. A rotating ring resonator CCW. The photonic crystal is at rest in the rotating reference frame.

written in the accelerating system frame of reference is more convenient for the study of the Sagnac effect discussed above and for the present application. Furthermore, in many actual implementations and usage of optical gyroscopes, an inertial frame of reference is not available (e.g., gyroscopes in navigation systems).

The structure of the paper is as follows. In Sec. II A, we study the RR-CCW at rest and establish the basic mathematical approach and physical quantities needed for the ensuing noninertial system study. The analysis is very similar to the one used in [5], with some modifications mainly in order to refrain from using variational principles used there, that hold for self-adjoint operators only. In Sec. II B, we extend the results to rotating systems, using the equations of electrodynamics in rotating media. In Sec. III, we discuss the application to optical gyroscopes.

II. Theory

A. System at rest

We shall start by a brief description of the system at rest: $\mathbf{\Omega}=\mathbf{0}$. We shall essentially follow the lines presented in [5], where the strong binding/weak coupling perturbation theory has been used to study the *linear* CCW at rest. We note that the variational solution procedure adopted in [5] holds only for self-adjoint operators. Since self-adjointness is lost due to rotation, and since the purpose of this subsection is to lay some of the mathematical foundations for the case of $\mathbf{\Omega} \neq \mathbf{0}$, we shall use here a solution procedure that does not rely on variational principles.

We assume that the PhC is made of a dielectric material with the permittivity $\epsilon=\epsilon_0\epsilon_r(\boldsymbol{r})$ and the constant vacuum permeability $\mu=\mu_0$. A time harmonic dependence $e^{-i\omega t}$ is assumed and suppressed. The magnetic field $\boldsymbol{H}$ is governed by the wave equation

$$\mathbf{\Theta}\boldsymbol{H} = (\omega/c)^2\boldsymbol{H}, \tag{2.1}$$

where $c=(\epsilon_0\mu_0)^{-1/2}$ is the speed of light in vacuum, and the operator $\mathbf{\Theta}$ is defined as

$$\mathbf{\Theta} = \nabla \times \frac{1}{\epsilon_r(\boldsymbol{r})} \nabla \times . \tag{2.1′}$$

As in [5], let the relative permittivity of the perfect periodic PhC be $\epsilon_p(\boldsymbol{r})$, and that of the PhC with the presence of a single, isolated microcavity located at the reference (defect) location $\boldsymbol{r}_0$ be $\epsilon_d(\boldsymbol{r}-\boldsymbol{r}_0)$. We define the reciprocal difference $d(\boldsymbol{r};\boldsymbol{r}_0)$,

$$d(\boldsymbol{r};\boldsymbol{r}_0) = \frac{1}{\epsilon_d(\boldsymbol{r}-\boldsymbol{r}_0)} - \frac{1}{\epsilon_p(\boldsymbol{r})}. \tag{2.2}$$

Define now the locations of the RR-CCW local defects as $\boldsymbol{r}_n$, $n=0,\ldots,M-1$, where M is the total number of the microcavities ($M=6$ in Figs. 2 and 3). Using Eq. (2.2), we have for the reciprocal of $\epsilon_r(\boldsymbol{r})$ (dielectric property of the entire structure)

$$\frac{1}{\epsilon_r(\boldsymbol{r})} = \frac{1}{\epsilon_p(\boldsymbol{r})} + \sum_{n=0}^{M-1} d(\boldsymbol{r};\boldsymbol{r}_n). \tag{2.3}$$

With this definition we can express $\boldsymbol{\Theta}$ as the sum of operators

$$\boldsymbol{\Theta} = \boldsymbol{\Theta}^{\text{per}} + \sum_{n=0}^{M-1} \boldsymbol{\Theta}_n, \tag{2.4}$$

where $\boldsymbol{\Theta}^{\text{per}}$ and $\boldsymbol{\Theta}_n$ are defined as in Eq. (2.1′) with $1/\epsilon_r(\boldsymbol{r})$ replaced by $1/\epsilon_p(\boldsymbol{r})$ and by $d(\boldsymbol{r};\boldsymbol{r}_n)$, respectively.

Let us denote now the magnetic field associated with the single, isolated microcavity at location $\boldsymbol{r}_n$, as $\boldsymbol{H}_n(\boldsymbol{r})$. It is a trapped mode. Since all the local defects are identical, they all resonate at the same frequency ω_0. We use the notation $\boldsymbol{H}_n(\boldsymbol{r}) = \boldsymbol{H}^{(0)}(\boldsymbol{r}-\boldsymbol{r}_n)$, where $\boldsymbol{H}^{(0)}(\boldsymbol{r})$ is the trapped mode as if the microcavity is located at the origin. These fields satisfy the eigenvalue equation

$$(\boldsymbol{\Theta}^{\text{per}} + \boldsymbol{\Theta}_n)\boldsymbol{H}_n = (\omega_0/c)^2 \boldsymbol{H}_n,$$
$$\text{Im}\,\boldsymbol{H}_n(\boldsymbol{r}) = 0, \quad n = 1,\ldots,M-1, \tag{2.5}$$

where $\boldsymbol{H}_n$ is the eigenfunction and $(\omega_0/c)^2$ is the eigenvalue. Note that since the differential operator in Eq. (2.5) is self-adjoint and all the equation coefficients are real, we can always normalize $\boldsymbol{H}_n(\boldsymbol{r})$ to be real. Since the $\boldsymbol{H}_n(\boldsymbol{r})$'s are highly localized within the isolated microcavities and decay exponentially outside them, and since the RR-CCW cavities are widely spaced, one can assume that the field within each of the cavities of the *entire* RR-CCW is essentially the same as the isolated cavity mode $\boldsymbol{H}_n(\boldsymbol{r})$. Thus, we expand the total field $\boldsymbol{H}(\boldsymbol{r})$ of the entire RR-CCW as a linear combination of the $\boldsymbol{H}_n$'s,

$$\boldsymbol{H}(\boldsymbol{r}) = \sum_{n=0}^{M-1} A_n \boldsymbol{H}_n(\boldsymbol{r}), \tag{2.6}$$

where the A_n's are unknown coefficients. We substitute Eq. (2.6) into the operator equation (2.1), and require that the expansion error be orthogonal to each of the expansion modes $\boldsymbol{H}_m(r)$,

$$\sum_{n=0}^{M-1} A_n \left[\langle \boldsymbol{\Theta}\boldsymbol{H}_n, \boldsymbol{H}_m \rangle - \left(\frac{\omega}{c}\right)^2 I_{n-m} \right] = 0, \quad m = 0,\ldots,M-1, \tag{2.7}$$

where

$$I_{n-m} \equiv \langle \boldsymbol{H}_n, \boldsymbol{H}_m \rangle \tag{2.7′}$$

and where $\langle \boldsymbol{F}, \boldsymbol{G} \rangle$ is the inner product between the vector functions $\boldsymbol{F}$ and $\boldsymbol{G}$, defined as

$$\langle \boldsymbol{F}, \boldsymbol{G} \rangle \equiv \int_V \boldsymbol{F} \cdot \overline{\boldsymbol{G}} dx\, dy\, dz. \tag{2.8}$$

Here $\overline{\boldsymbol{G}}$ is the complex conjugate of $\boldsymbol{G}$, and the dot denotes the conventional Cartesian scalar product between two vectors. The integration domain extends over the entire three-dimensional space. Using now Eqs. (2.4) and (2.5), we obtain

$$\sum_{n=0}^{M-1} A_n [(\omega_0^2 - \omega^2) I_{n-m} + c^2 \tau_{n-m}] = 0, \quad m = 0,\ldots,M-1, \tag{2.9}$$

where

$$\tau_{n-m} = \sum_{k \neq n} \langle \boldsymbol{\Theta}_k \boldsymbol{H}_n, \boldsymbol{H}_m \rangle. \tag{2.9′}$$

Note that I_{n-m}, τ_{n-m} depend only on the distance $\boldsymbol{r}_n - \boldsymbol{r}_m$, and they decrease exponentially when this distance increases. In principle, these terms are completely equivalent to their "linear" counterparts in the linear CCW problem studied in [5]. Thus, we can follow [5] and suggest the solution

$$A_n = e^{i\kappa n}. \tag{2.10}$$

We substitute this solution back into Eq. (2.9). Note that since the local modes $\boldsymbol{H}_n(\boldsymbol{r})$ are highly localized around $\boldsymbol{r} = \boldsymbol{r}_n$, I_n, $n \neq 0$ is exponentially smaller than I_0. Likewise, $\tau_1 = \tau_{-1}$ are the dominant terms between the τ_n. See [5] for technical details. Using the equation shift-invariance property, and collecting only the dominant terms, we are left with the dispersion relation (see [5])

$$\omega^2 - \omega_0^2 = 2c^2 \tau_1 \|\boldsymbol{H}_0\|^{-2} \cos(\kappa), \tag{2.11}$$

where $\|\boldsymbol{H}_0\|^2 = \langle \boldsymbol{H}_0, \boldsymbol{H}_0 \rangle = I_0$. Simplifying one step further by $\omega^2 - \omega_0^2 \approx 2\omega_0(\omega - \omega_0)$, we get

$$\omega(\kappa) = \omega_0 + \Delta\omega \cos(\kappa), \quad \Delta\omega = c^2 \tau_1 / (\omega_0 \|\boldsymbol{H}_0\|^2). \tag{2.11′}$$

This dispersion relation is completely analogous to the dispersion obtained in [5]. However, since the structure here is periodic with respect to rotation, the relation $A_n/A_{n-1} = e^{i\kappa}$ that holds for all $0 \leqslant n \leqslant M-1$ should hold also between the terms $n = M-1$ and $n = 0$. Thus

$$e^{i\kappa(M-1)} e^{i\kappa} = 1 \Rightarrow \kappa = \kappa_m = 2\pi m/M,$$
$$m = 0, \pm 1, \pm 2, \ldots, \pm (M-1). \tag{2.12}$$

This condition selects $2M-1$ points on the continuous dispersion curve of Eqs. (2.11) and (2.11′). Note that positive or negative values of κ correspond to counterclockwise or clockwise propagation, respectively. However, since Eq. (2.11) is even with respect to κ, the two opposing propagation directions possess exactly the same frequency characteristics.

B. The rotating system

Let the entire PhC rotate at angular velocity $\boldsymbol{\Omega}$ around the center of our RR-CCW, as shown in Fig. 3. The system is at rest in the noninertial reference frame $\mathcal{R}:(x',y',z')$. Without loss of generality, we assume that the rotation is around z, so we have

$$\mathbf{\Omega} = \hat{\mathbf{z}}\Omega_0, \tag{2.13a}$$

where Ω_0 is a scalar measuring the angular velocity magnitude; it possesses a positive or negative sign for counterclockwise or clockwise rotations, respectively. Thus,

$$\begin{pmatrix} x' \\ y' \\ z' \end{pmatrix} = \begin{pmatrix} \cos(\Omega_0 t) & \sin(\Omega_0 t) & 0 \\ -\sin(\Omega_0 t) & \cos(\Omega_0 t) & 0 \\ 0 & 0 & 1 \end{pmatrix} \begin{pmatrix} x \\ y \\ z \end{pmatrix} \tag{2.13b}$$

and the RR-CCW lies on the x', y' plane.

Our purpose now is to solve Maxwell's equations in the rotating system $\mathcal{R}$. Some important points are observed.

(i) In $\mathcal{R}$, the system properties do not vary in time.

(ii) The angular velocity Ω_0 and the PhC maximal dimension L satisfy $|\Omega_0 L| \ll c$. Therefore, no relativistic effects take place.

(iii) Consistent with the slow velocity assumption above, no geometrical transformations or deformations take place. Thus, for example, the ∇ operator is conserved: $\nabla = \nabla'$. For the very same reason, time is invariant in both systems: $t = t'$.

According to the formal structure of electrodynamics, the basic physical laws are invariant under *all* space-time transformations (including noninertial ones). Therefore, the source-free Maxwell's equations in $\mathcal{R}$ are given by [8,9]

$$\nabla' \times \boldsymbol{E}' = i\omega \boldsymbol{B}', \quad \nabla' \cdot \boldsymbol{B}' = \mathbf{0}, \tag{2.14a}$$

$$\nabla' \times \boldsymbol{H}' = -i\omega \boldsymbol{D}', \quad \nabla' \cdot \boldsymbol{D}' = \mathbf{0}. \tag{2.14b}$$

The transformation from the inertial system $\mathcal{I}$ to the rotating one $\mathcal{R}$ is manifested via the local constitutive relations. Let the material properties at rest be given by ϵ, μ. Then up to the first order in velocity, the constitutive relations in $\mathcal{R}$ take on the form [9]

$$\boldsymbol{D}' = \epsilon \boldsymbol{E}' - c^{-2}\mathbf{\Omega} \times \boldsymbol{r}' \times \boldsymbol{H}', \tag{2.15a}$$

$$\boldsymbol{B}' = \mu \boldsymbol{H}' + c^{-2}\mathbf{\Omega} \times \boldsymbol{r}' \times \boldsymbol{E}'. \tag{2.15b}$$

Substituting into Eqs. (2.14a) and (2.14b), Maxwell's equations become

$$\mathrm{D} \times \boldsymbol{E}' = i\omega\mu \boldsymbol{H}', \tag{2.16a}$$

$$\mathrm{D} \times \boldsymbol{H}' = -i\omega\epsilon \boldsymbol{E}', \tag{2.16b}$$

where $\mathcal{D}$ is the operator,

$$\mathrm{D} \equiv \nabla' - ik\boldsymbol{\beta}(\boldsymbol{r}'), \quad k = \omega/c, \quad \boldsymbol{\beta}(\boldsymbol{r}') = c^{-1}\mathbf{\Omega} \times \boldsymbol{r}'. \tag{2.17}$$

We follow now the standard procedure of deriving the wave equation for $\boldsymbol{H}'$, with $\mathcal{D}$ replacing ∇. The resulting equation is $\mathcal{D} \times (1/\epsilon_r)\mathcal{D} \times \boldsymbol{H}' = k^2 \boldsymbol{H}'$. Collecting terms that are first order only (with respect to velocity,) and rearranging, we end up with the new wave equation

$$\mathbf{\Theta}' \boldsymbol{H}' = k^2 \boldsymbol{H}' + ik\left(\nabla' \times \frac{1}{\epsilon_r}\boldsymbol{\beta}(\boldsymbol{r}') \times \boldsymbol{H}' + \frac{1}{\epsilon_r}\boldsymbol{\beta}(\boldsymbol{r}') \times \nabla' \times \boldsymbol{H}' \right). \tag{2.18}$$

This is the new wave equation that has to be solved. Here $\mathbf{\Theta}'$ is defined the same as $\mathbf{\Theta}$ in Eq. (2.1′), but with the unprimed coordinates replaced by the primed ones. The difference between this equation, and the equation of the system at rest 2.1, is only in the introduction of the additional terms multiplied by ik on the right-hand side. It has been shown in [2] that the effect of rotation on the modal shape of the field is generally completely negligible. The major contribution of the Sagnac effect is manifested in the phase property of the field. Thus, motivated by the expansion of the field in the system at rest, we use now exactly the same expansion,

$$\boldsymbol{H}'(\boldsymbol{r}') = \sum_{n=0}^{M-1} A_n \boldsymbol{H}_n(\boldsymbol{r}'), \quad \boldsymbol{H}_n(\boldsymbol{r}') = \boldsymbol{H}_0(\boldsymbol{r}' - \boldsymbol{r}_n'), \tag{2.19}$$

where the Sagnac effect is expressed essentially through the modal amplitudes and phases, i.e., through the A_n's. Furthermore, for the very same reasons, the solution procedure used in the previous section applies here as well. It should be emphasized that the expansion functions $\boldsymbol{H}_n$ are treated as pure mathematical entities; these are not field quantities that must obey electrodynamics laws [their sum according to Eq. (2.19) should]. Since $\nabla = \nabla'$ [see item (iii) above], we have

$$\left(\mathbf{\Theta}'^{\mathrm{per}} + \mathbf{\Theta}_n'\right)\boldsymbol{H}_n(\boldsymbol{r}') = k_0^2 \boldsymbol{H}_n(\boldsymbol{r}'), \quad k_0 = \omega_0/c. \tag{2.20}$$

Substituting Eq. (2.19) into Eq. (2.18), and following exactly the same procedure executed in Sec. II A, we end up with an equation similar to Eq. (2.7), but with correction terms F_{nm},

$$\sum_{n=0}^{M-1} A_n[\langle \mathbf{\Theta}' \boldsymbol{H}_n, \boldsymbol{H}_m \rangle - k^2 I_{n-m}] = ik \sum_{n=0}^{M-1} A_n F_{nm}, \quad m = 0, \ldots, M-1, \tag{2.21}$$

where I_{n-m} is defined as in Eq. (2.7′), the inner product is defined similarly to that in $\mathcal{I}$, and

$$F_{nm} = \left\langle \nabla' \times \frac{\beta}{\epsilon_r} \times \boldsymbol{H}_n, \boldsymbol{H}_m \right\rangle + \left\langle \frac{\beta}{\epsilon_r} \times \nabla' \times \boldsymbol{H}_n, \boldsymbol{H}_m \right\rangle, \tag{2.21′}$$

and where $\boldsymbol{\beta} = \boldsymbol{\beta}(\boldsymbol{r}')$ and k are defined as in Eq. (2.17). After some algebraic vector manipulations, we can rewrite F_{nm} as follows (see the Appendix for details):

$$F_{nm} = \begin{cases} 0, & n = m \\ 2\left(\frac{\Omega_0}{c}\right) q_{n-m}, & n \neq m, \end{cases} \tag{2.22}$$

where q_{n-m} is given by

$$q_{n-m} = \left\langle \frac{|\boldsymbol{r}'|}{\epsilon_r}\hat{\boldsymbol{\phi}}', \boldsymbol{H}_n \times \nabla' \times \boldsymbol{H}_m \right\rangle = -q_{m-n}. \quad (2.22')$$

Substituting this back into Eq. (2.21), using Eq. (2.20), and recalling that $\boldsymbol{\Theta}'$ can be decomposed as in Eq. (2.4), we obtain

$$\sum_{n=0}^{M-1} A_n[(\omega_0^2 - \omega^2)I_{n-m} + c^2\tau_{n-m}] = i2\omega\Omega_0 \sum_{n,n\neq m}^{M-1} A_n q_{n-m},$$
$$m = 0,\ldots,M-1, \quad (2.23)$$

which is the "rotating counterpart" of Eq. (2.9). As with the static problem, the coefficients here depend only on the distance $\boldsymbol{r}_n - \boldsymbol{r}_m$, and decrease exponentially as this distance increases. Thus, we assume a solution of the form of Eq. (2.10), and follow exactly the same steps. The result is the following Ω_0-dependent dispersion relation:

$$\omega^2 - \omega_0^2 = 2c^2\tau_1\|\boldsymbol{H}_0\|^{-2}\cos(\kappa) + 4\omega\Omega_0 q_1\|\boldsymbol{H}_0\|^{-2}\sin\kappa. \quad (2.24)$$

Assuming again that $\omega \approx \omega_0$ (as with the stationary system), and slow rotations, this result can be rewritten as

$$\omega(\kappa) = \omega_0 + \Delta\omega\cos(\kappa - \Omega_0 Q), \quad (2.25)$$

where the bandwidth $\Delta\omega$ is identical to that of the stationary CCW given in Eq. (2.11′), Q is given by

$$Q = 2\omega_0 q_1/(c^2\tau_1), \quad (2.25')$$

and it is noteworthy that we still have the 2π periodicity requirement, for which the selection rule in Eq. (2.12) holds.

The last result is the dispersion curve we sought after. Unlike the stationary system, the curve is not symmetric around the origin of the κ axis. Clockwise and counterclockwise propagations differ in frequency, due to the shift $\Omega_0 Q$, which depends linearly on the rotation frequency. The curves of the stationary and rotating systems are shown in Fig. 4.

III. The Photonic Crystal Optical Gyroscope

Using Eq. (2.25), it is seen that the beat frequency obtained when both clockwise and counterclockwise propagations are present is given by ($\kappa_{-m} = -\kappa_m$)

$$\omega_b = \omega(\kappa_m;\Omega_0) - \omega(-\kappa_m;\Omega_0) = 2\Delta\omega\sin(\omega_0 Q)\sin(2m\pi/M). \quad (3.1)$$

Assuming that M is large, the maximal beat frequency is obtained when $\sin(2m\pi/M) \approx 1$. Thus, for slow rotations we obtain

$$\omega_b = 2\Omega_0\Delta\omega Q, \quad (3.2)$$

where Q is given in Eq. (2.25′).

While the results of the previous section characterize the system dynamics, the relevant parameters q_1, τ_1, and consequently Q are given in terms of operators on field quantities that are not easily calculated. It is most desirable to get an estimate for Q using physical quantities that are easier to compute or to measure. Towards this end, we use Eq. (2.11′)

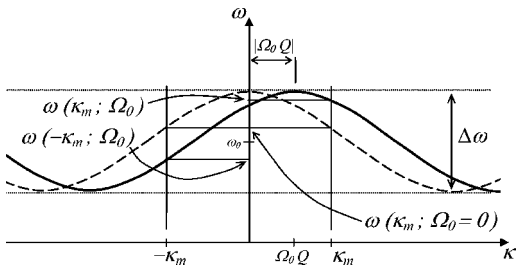

FIG. 4. Dispersion curves of the stationary system (dashed line) and rotating system (solid line) in their rest frame of reference. In the stationary system, we have $\omega(\kappa_m) = \omega(-\kappa_m)$. In the rotating system, they split into two different frequencies as shown.

to express τ_1 in terms of the system bandwidth (identical in $\mathcal{I}$ and in $\mathcal{R}$), and substitute it in the expression for Q [see Eq. (2.25′)]. With this, the expression for ω_b becomes

$$\omega_b = 4\Omega_0 q_1\|\boldsymbol{H}_0\|^{-2}. \quad (3.3)$$

Furthermore, assuming that the RR-CCW radius R is large compare to the microcavity dimensions (see Fig. 3), and recalling that the microcavity field $\boldsymbol{H}_n(r')$ is highly localized within it, q_1 can be approximated as

$$q_1 \approx R\langle\epsilon_r^{-1}\hat{\boldsymbol{\phi}}, -\boldsymbol{H}_1 \times i\omega_0\epsilon_{d_n}\boldsymbol{E}_0\rangle, \quad (3.4)$$

where $\epsilon_{d_n} = \epsilon_d(\boldsymbol{r} - \boldsymbol{r}_n)$ with the latter defined after Eq. (2.1′).

Some observations are made now.

(i) Since $\boldsymbol{E}_0, \boldsymbol{H}_0$ are the mode functions of isolated microcavity, their mutual Poynting vector does not carry real power. Power flow in the CCW is only due to terms of the form $\mathrm{Re}\,\boldsymbol{E}_0 \times \boldsymbol{H}_1$. Therefore, the second quantity in the inner product in Eq. (3.4) is larger than, or equal to, the volume average (over a CCW microcavity) of $\epsilon_{d_n} S$, where S is the net real power that flows along the circular path.

(ii) The total electromagnetic power stored in a microcavity volume is $1/2(\epsilon\|\boldsymbol{E}_0\|^2 + \mu\|\boldsymbol{H}_0\|^2)$. However, all cavities are close to resonance; the electric and magnetic stored energies are equal. Hence, the total electromagnetic power stored in the volume of each microcavity is $U = \mu_0\|\boldsymbol{H}_0\|^2$.

(iii) The group velocity v_g is given by the ratio of the (averaged over medium period) power flow S to the stored energy U [13].

With the observations above and with Eq. (3.4), it is now straightforward to show that

$$q_1\|\boldsymbol{H}_0\|^{-2} \geqslant R v_g \omega_0/c^2, \quad (3.5)$$

where R is the RR-CCW radius (see Fig. 3). At the point of maximal beat frequency ($\kappa_m \approx \pi/2$), we also have (see the dispersion curve in Fig. 4) $v_g = \Delta\omega\, b$, where b is the intercavity spacing, shown in Fig. 3. Thus we get from Eq. (3.5)

$$\omega_b \geqslant 4\Omega_0 R\, b\, \Delta\omega\, \omega_0 c^{-2}. \quad (3.6)$$

This last result is a rough estimate of the beat frequency due to rotating RR-CCW in photonic crystals. New parameters, not present in classical studies of the Sagnac effect, determine the beat frequency: system bandwidth and intercavity spacing.

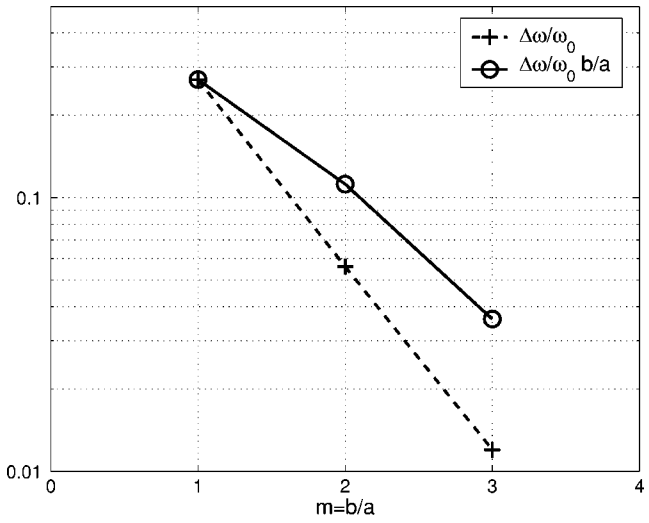

FIG. 5. Typical values for relative bandwidth $\Delta\omega/\omega_0$ and $(\Delta\omega/\omega_0)$ (b/a) vs b/a for a CCW in a PhC with hexagonal symmetry (after [5]).

It should be recognized, however, that $\Delta\omega$ and b cannot be chosen freely and independently. In fact, it has been shown that $\Delta\omega$ decreases *exponentially* when b increases [5]. This can be seen also in Eqs. (2.9′) and (2.11′): since the microcavity mode $\boldsymbol{H}_0$ is exponentially decreasing, and since τ_1 in Eq. (2.9′) consists of essentially an overlapping integral of the fields in two neighboring microcavities, the resulting $\Delta\omega$ must decrease fast when b is increased. Indeed, a typical example of the dependence between $\Delta\omega$ and b, normalized with respect to the length of the PhC primitive lattice vector a, is shown in Fig. 5 (see [5] for details).

For an operating wavelength of about 1 μm, the primitive lattice vector a has a length of about 0.5 μm (Bragg condition). Using the data of Fig. 5, it is seen that for a CCW with intercavity spacing of two lattice cells ($m=2$), we have $\Delta\omega\, b/(\omega_0 a)\approx 1.1$. Using now Eq. (3.6) with the values above, we obtain $\omega_b \approx 1.6\times 10^8 \times R\,\Omega_0$. For RR-CCW with a radius of about 1 mm, this yields $\omega_b \approx 1.6\times 10^5 \Omega_0$.

In implementing the Sagnac effect to optical gyroscopes, care should be taken to design the clockwise and counterclockwise propagation paths as reciprocal as possible for $\Omega_0=0$ [1]. Since the RR-CCW has an extremely small footprint, environmental conditions across the structure should not vary significantly, thus we anticipate that the requirement for reciprocity (at rest) of the two circulating paths can be maintained relatively easily. The only parameter that seems to demand more care during the design of the optical gyroscope is the reciprocity of the optical couplings in and out. Two design possibilities, using linear CCW's as a means to guide the optical signal, are shown in Fig. 6.

Another point worth mentioning regarding practical implementation is that structural disorder resulting from design and fabrication inaccuracies may formally affect the CCW's and RR-CCW's operation. However, it has been shown in [6] that the CCW's sensitivity with respect to structural disorder possesses a thresholdlike character; it is practically insensitive to disorder if the latter is below a certain level, but it may cease to operate if the disorder exceeds this level. This threshold has been fully characterized and studied in [6].

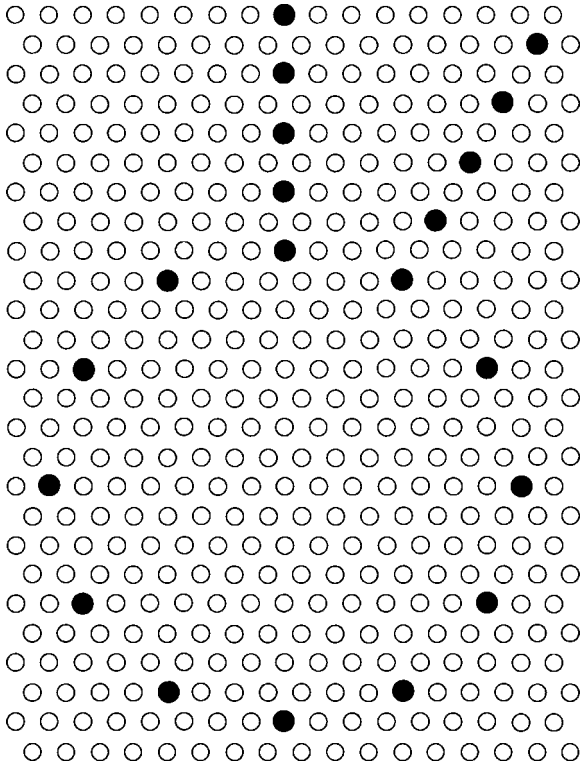

FIG. 6. RR-CCW with two possible designs for reciprocal coupling of the optical signal using linear CCW's.

IV. Conclusions

Using the equations of electrodynamics in rotating media, we have studied the effect of rotation on the propagation of waves in a photonic-crystal-based coupled-cavity waveguide. Using a perturbation approach, a novel manifestation of the Sagnac effect in photonic crystals has been investigated and demonstrated. This effect can be used to design very compact optical gyroscopes.

ACKNOWLEDGMENTS

The author would like to thank M. Tur for a stimulating discussion on the subject.

Appendix A: The F_{nm} coefficients

We have the following identities [use $(\nabla\times\boldsymbol{A})\cdot\boldsymbol{B}=\nabla\cdot(\boldsymbol{A}\times\boldsymbol{B})+\boldsymbol{A}\cdot(\nabla\times\boldsymbol{B})$, and $\boldsymbol{A}\cdot(\boldsymbol{B}\times\boldsymbol{C})=(\boldsymbol{A}\times\boldsymbol{B})\cdot\boldsymbol{C}$]:

$$\left[\nabla'\times\frac{\beta}{\epsilon_r}\times\boldsymbol{H}_n\right]\cdot\boldsymbol{H}_m=\nabla'\cdot\left[\left(\frac{\beta}{\epsilon_r}\times\boldsymbol{H}_n\right)\times\boldsymbol{H}_m\right]+\left(\frac{\beta}{\epsilon_r}\times\boldsymbol{H}_n\right)\cdot(\nabla'\times\boldsymbol{H}_m), \tag{A1a}$$

$$\left[\frac{\beta}{\epsilon_r}\times\nabla'\times\boldsymbol{H}_n\right]\cdot\boldsymbol{H}_m=-\left(\frac{\beta}{\epsilon_r}\times\boldsymbol{H}_m\right)\cdot(\nabla'\times\boldsymbol{H}_n). \tag{A1b}$$

The inner products of F_{nm} in Eq. (2.21′) are nothing but volume integrations (over arbitrarily large volume V) of the above terms. Using the Gauss theorem, we get for the contribution of the first term on the RHS of Eq. (A1a),

$$\int_V \nabla'\cdot\left[\left(\frac{\beta}{\epsilon_r}\times\boldsymbol{H}_n\right)\times\boldsymbol{H}_m\right]d^3x' = \oint_{S=\partial V}\left[\left(\frac{\beta}{\epsilon_r}\times\boldsymbol{H}_n\right)\times\boldsymbol{H}_m\right]\cdot ds\to 0. \tag{A2}$$

This is because the flux through the surface $S=\partial V$ vanishes as V becomes very large (the functions $\boldsymbol{H}_n$ are exponentially decreasing). Therefore, F_{nm} eventually comprises

$$F_{nm}=\left\langle\frac{\beta}{\epsilon_r}\times\boldsymbol{H}_n,\nabla'\times\boldsymbol{H}_m\right\rangle-\left\langle\frac{\beta}{\epsilon_r}\times\boldsymbol{H}_m,\nabla'\times\boldsymbol{H}_n\right\rangle. \tag{A3}$$

Using again $(\boldsymbol{A}\times\boldsymbol{B})\cdot\boldsymbol{C}=\boldsymbol{A}\cdot(\boldsymbol{B}\times\boldsymbol{C})$,

$$F_{nm}=\left\langle\frac{\beta}{\epsilon_r},\boldsymbol{H}_n\times\nabla'\times\boldsymbol{H}_m\right\rangle-\left\langle\frac{\beta}{\epsilon_r},\boldsymbol{H}_m\times\nabla'\times\boldsymbol{H}_n\right\rangle = \begin{cases}0, & n=m\\ 2\dfrac{\Omega_0}{c}q_{n-m}, & n\neq m,\end{cases} \tag{A4}$$

where, with $\boldsymbol{\beta}=\Omega_0\hat{\boldsymbol{z}}\times\boldsymbol{r}'/c=\Omega_0|\boldsymbol{r}'|\hat{\boldsymbol{\phi}}'/c$ and with the obvious symmetries,

$$q_{n-m}\equiv\left\langle\frac{|\boldsymbol{r}'|}{\epsilon_r}\hat{\boldsymbol{\phi}}',\boldsymbol{H}_n\times\nabla'\times\boldsymbol{H}_m\right\rangle=-q_{m-n}. \tag{A.4′}$$

[1] *Fiber-Optic Rotation Sensors*, edited by S. Ezekiel and H. J. Arditty Springer Series In Optical Sciences (Springer-Verlag, Berlin, 1982).
[2] H. J. Arditty and H. C. Lefevre, Opt. Lett. **6**, 401 (1981).
[3] H. C. Lefevre, Opt. Rev. **4**, 20 (1997).
[4] A. Yariv, Y. Xu, R. K. Lee, and A. Scherer, Opt. Lett. **24**, 711 (1999).
[5] A. Boag and Ben Z. Steinberg, J. Opt. Soc. Am. A **18**, 2799 (2001).
[6] Ben. Z. Steinberg, A. Boag, and R. Lisitsin, J. Opt. Soc. Am. A **20**, 138 (2003).
[7] Ben Z. Steinberg (unpublished).
[8] J. L. Anderson and J. W. Ryon, Phys. Rev. **181**, 1765 (1969).
[9] T. Shiozawa, Proc. IEEE **61**, 1694 (1973).
[10] M. Skorobogatiy and J. D. Joannopoulos, Phys. Rev. B **61**, 5293 (2000).
[11] M. Skorobogatiy and J. D. Joannopoulos, Phys. Rev. B **61**, 15 554 (2000).
[12] E. J. Reed, M. Soljacic, and J. D. Joannopoulos, Phys. Rev. Lett. **90**, 203904 (2003).
[13] A. Yariv and P. Yeh, *Optical Waves in Crystals* (Wiley, New York, 1984).